American Journal of Mechanical and Materials Engineering
2018; 2(2): 15-20
http://www.sciencepublishinggroup.com/j/ajmme
doi: 10.11648/j.ajmme.20180202.11

Effects of Laser Shock Peening on Mechanical Properties and Surface Morphology of AA2024 Alloy

Samuel Adu-Gyamfi[1, *], Philip Agyepong Boateng[1], Enoch Asuako Larson[2], Philip Yamba[2], Anthony Akayeti[2]

[1]Department of Mechanical Engineering, Sunyani Technical University, Sunyani, Ghana

[2]Department of Mechanical Engineering, Tamale Technical University, Tamale, Ghana

Email address:
aristotle818@yahoo.com (S. Adu-Gyamfi)

[*]Corresponding author

To cite this article:
Samuel Adu-Gyamfi, Philip Agyepong Boateng, Enoch Asuako Larson, Philip Yamba, Anthony Akayeti. Effects of Laser Shock Peening on Mechanical Properties and Surface Morphology of AA2024 Alloy. *American Journal of Mechanical and Materials Engineering*. Vol. 2, No. 2, 2018, pp. 15-20. doi: 10.11648/j.ajmme.20180202.11

Received: May 29, 2018; **Accepted**: June 21, 2018; **Published**: July 21, 2018

Abstract: This paper presents the after effect of laser shock peening (LSP) on AA2024 alloy specimen irradiated with the L-Spiral scanning pattern at different pulse energies. The surface morphology indicates an increase in surface roughness after LSP. The X-Ray diffraction analysis of the LSP treated specimens were compared with the untreated specimen. The $\sin^2\Psi$ method of the X-ray diffraction technique indicates an improvement in the magnitude of compressive residual stress distribution after LSP. The hardness profile after LSP also shows substantial increment. The results suggested an improvement in the microstructural structure owing to the ultra-high strain rate deformation and refined grains. The High Score Plus software is used to analyse the crystallite size and microstrain of the alloy treated by different pulse energies.

Keywords: Laser Shock Peening, Residual Stress Distribution, Laser Pulse Energy, Surface Morphology, AA2024 Alloy

1. Introduction

After high power lasers were developed, attention has shifted to laser surface modification processes and one of the applications growing rapidly is laser shock peening (LSP). LSP is an innovative surface treatment method which has widely been used to enhance the performances and defects of many automobile and other engineering components [1-5]. LSP is capable of improving the surface and mechanical properties with short pulse (ns level) and high peak power laser beam density (GW/cm^2) to generate a plasma at high pressure to induce compressive residual stress layer on the surfaces of metallic materials [3, 6, 7]. Surface is the outermost layer of the material which is in contact with other materials. Hence, it is essential for us to know the properties of the surfaces of metallic materials to upgrade them for the rationalisation of their mechanical properties to guarantee the long life of the materials. It is highly important to know about the surface because most of cracks and failure modes develop from the surface of the material and then propagate within the material, thus giving birth to fatigue. Aluminium alloy has been widely used in automotive and aerospace industries owing to their moderate strength and light weight [8]. Considerable studies have been done to examine the effects of LSP on both mechanical properties and fatigue live enhancement on aluminium alloys [2, 9-11]. It has been indicated by most of the researches that LSP improves the mechanical properties and fatigue life of aluminium alloys significantly owing to the compressive residual stresses. However, few studies have been focused on the effects of LSP with different energies on the surface morphology and mechanical properties with reference to the laser irradiating scanning pattern.

2. Materials and Methods

2.1. Material Properties and Sample Preparations

The AA2024-T351 was machined as a square shape with dimensions 20 x 20 mm and 3 mm thickness. Typical chemical composition and mechanical properties of the material is shown in Table 1 and 2 respectively. Figure 1 shows the composition of elements in the aluminium material

used during the experiment. Before LSP the specimens were polished with silicon carbide sandpaper in ascending order off grit size 400, 600, 800, 1200 and 4000 with water as polishing medium. It was finally polished with diamond paste with lubricated liquid on cloth paper followed by cleaning with distilled water. Ethanol was used to degrease the specimen surface. The L-Spiral scanning advancing pattern was employed in irradiating laser on the surface of the specimen. The specimens were treated by a single impact with different laser pulse energies of 4 J and 6 J, respectively.

Table 1. *Chemical composition of aluminium alloy 2024-T351 (wt %).*

Elements	Cu	Mg	Si	Fe	Mn	Other	Al
Composition	4.5	1.6	0.5	0.5	0.7	0.5	Bal.

Table 2. *Mechanical properties of aluminium alloy 2024-T351.*

Mechanical property	Tensile Strength (MPa)	Yield Strength (MPa)	Elongation (d,%)	Elasticity Modulus (GPa)	Poisson Ratio
Value	421.8	307.0	19.6	72.4	0.33

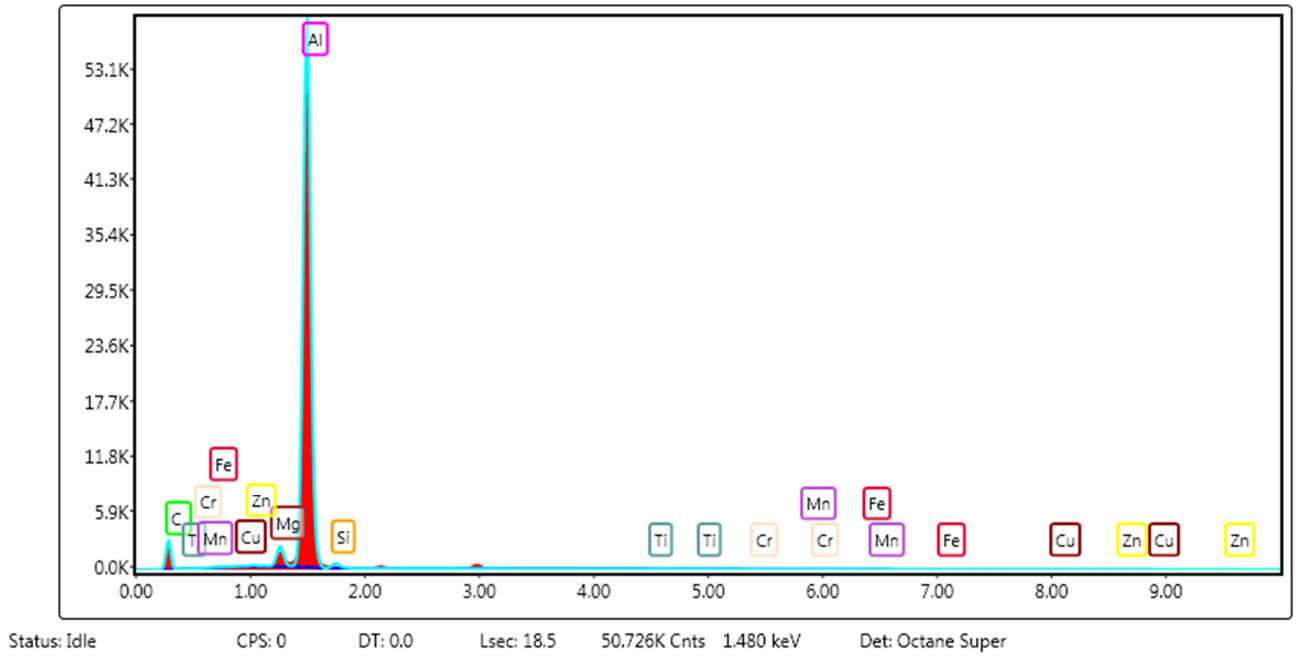

Figure 1. *Chemical composition of aluminium alloy 2024-T351.*

2.2. Laser Shock Peening

During LSP experiment, shockwaves generated by a plasma medium induces compressive residual stress on the surface of the specimen. A thin layer of absorbent coating (between 30-40 μm thickness and mostly of commercial black paint [12]) is coated on the surface of the work piece to serve as a sacrificial material to absorb most of the laser energy and prevent the workpiece from direct thermal contact from the laser induced. Water which serves as a transparent confining layer flows on top of the work piece to protect it from thermal effect. A Q-switched ND-YAG laser operating at a wavelength of 1064 nm, a pulse duration of 10 ns at FWHM with a high intensity pulsed laser beam of 4J or 6J deduced from the empirical equation of the laser induced shock pressure, $P(GPa) = 0.01\sqrt{\frac{\alpha}{2\alpha+3}}\sqrt{Z}\sqrt{I_o}$, where α is the portion of absorbed energy that contribute to the thermal energy of the plasma, Z is the reduced shock impedance between the targeted material and confining medium and I_o as the laser intensity. A power densities of more than 1 GW/cm^2 is directed unto the surface of the specimen [13, 14]. During the LSP process, the beam was directed perpendicular to the specimen surface, and the water layer was replaced after each line of impact to keep the water pure and to avoid water bubble formation or impurities coming from the material ablation. The absorbent material absorbs the laser energy, ionizes to plasma and expands between the absorbent material and confining media leading to the shockwave propagation into the specimen. When the plasma pressure of the shockwave exceeds the dynamic yield strength or HEL (Hugoniot Elastic Limit) of the material, the material undergoes extremely high strain-rate deformation of about 10^6-$10^7 s^{-1}$ during a short time and induces local plastic deformation in the material generating compressive residual stresses [15]. The overlapping rate, the distance, d between two adjacent spots was 50% as shown in Figure 3. All LSP processing parameters is tabulated in Table 3.

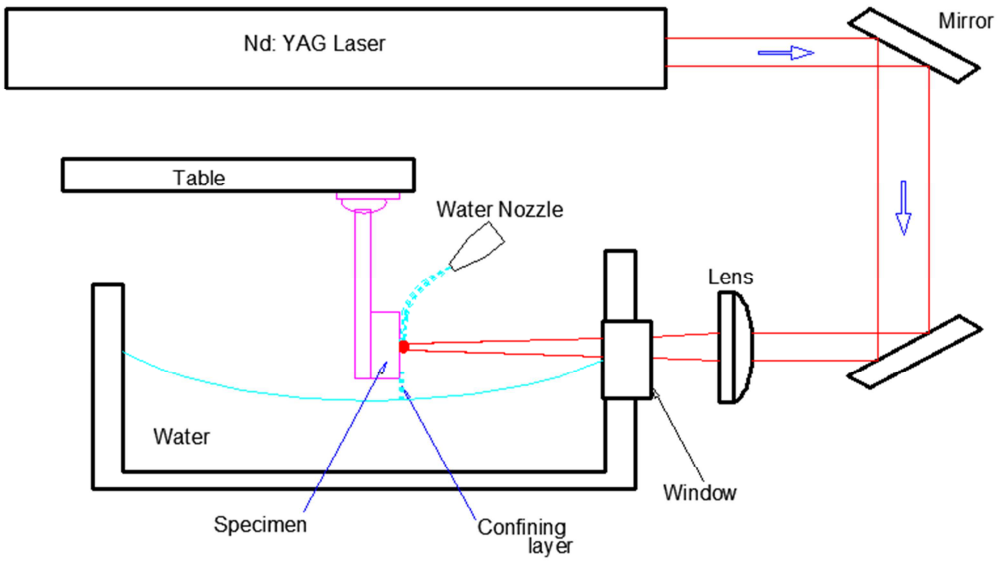

Figure 2. *Experimental set up of laser shock peening process.*

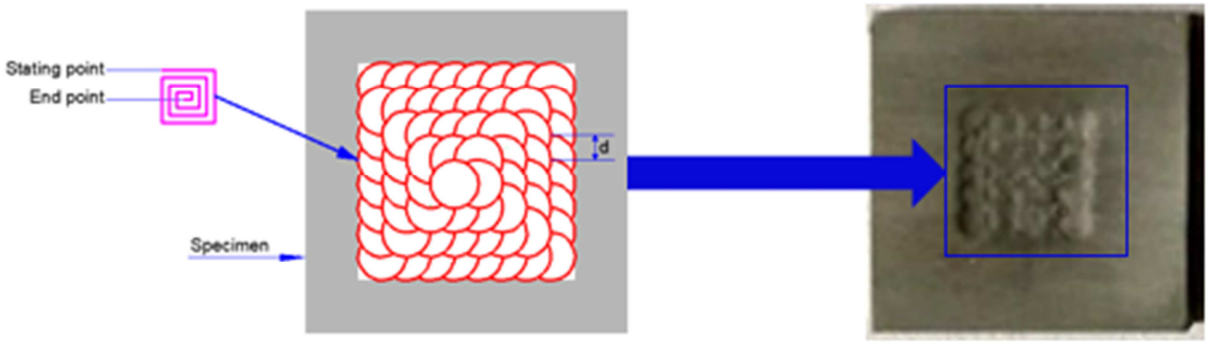

Figure 3. *Irradiating L-Spiral scanning pattern and the specimen treated with LSP.*

Table 3. *Laser shock peening processing parameters.*

Processing parameter	Pulse energy (J)	Spot diameter (mm)	Pulse width (ns)	Overlapping rate (%)	Laser wavelength (nm)
Value	4 & 6	3	10	50	1064

2.3. XRD

In studying the effect of LSP on the aluminium alloy, the XRD method was used to analyze the various diffraction patterns by the untreated and single impact. The XRD pattern of the specimens were recorded with Cu-Kα radiation at a frequency of λ = 1.5406 Å within a range of 2θ from 30 ^{o} to 120 ^{o} at a speed of 5^{o}/min.

2.4. Residual Stress

The X-ray diffraction with sin2Ψ method is used in this work to measure the residual stresses of the aluminium alloy before and after LSP. The Ψ was set to 0^{o}, 25^{o}, 35^{o} and 45^{o} respectively. The X-ray light tube voltage and current were set 22.0 kV and 6.0 mA, respectively. Counting time was 0.50 s. The X-ray beam diameter was 1 mm. The X-ray sources is CuKα ray and the diffraction plane is α phase (311) plane. The stress constant K was -166 MPa/(^{o}), The feed angle of the ladder scanning was 0.2^{o}/s. The scanning starting angle and ending angle were 130^{o} and 143^{o}, respectively. Samples were removed layer by layer via electrolytic polishing to obtain the depth profile of the residual stress.

2.5. Microhardness Characterisation

Hardness is a physical property of a material that enables it to resist bending, scratching, abrasion or any plastic deformation. The micro-hardness test was performed by Vickers hardness machine (HXD-1000TMSC/LCD). The hardness testing was performed in accordance with ASTM Standard E92-82 [16].

2.6. Surface Topography and Roughness

The surface topographical measurements, both two and three dimensional surface topography were investigated using Axio CSM 700 confocal laser scanning microscope. The optics allow topographical measurements at up to 117 frames per second. It is able to focus and detect from a step height at 20 nm up to the millimeter range.

3. Results and Discussion

3.1. XRD Analysis

Figure 4 shows the XRD patterns of specimens treated by LSP at different energies. It is evident from the figure that no new peaks are formed after laser impacts on the specimens for both energies. It is also obvious that there is no phase transformation in the surface layer of the aluminium alloy treated by LSP. However, it can be observed that the diffraction peaks of the laser treated specimen are broader than the untreated specimen, indicating refined grains and dislocation tangles. The specimen treated by 6 J pulse energy were broader compared to the specimens treated by 4 J. This is as a result of high plastic strain deformation and micro-strain among adjacent peaks as the laser energy increases. There is an increase in micro-stress in the surface layer of the alloy and/ or an increase in the crystal lattice distortion [17, 18] as a result of the dislocation multiplication after LSP. The High Score Plus software was used to analysed the crystallite size of the alloy. The grain size of the untreated specimen is at least 125.4 nm. The grain size after the specimen was treated with a single laser impact indicates grain refinement at 4 J (109.9 nm) and 6 J (95.9 nm) for a microstrain of 4 J (0.07378 %) and 6 J (0.07599%) respectively. As shown in Figure 5 coarse grains are refined after LSP, meaning the grains are compressed.

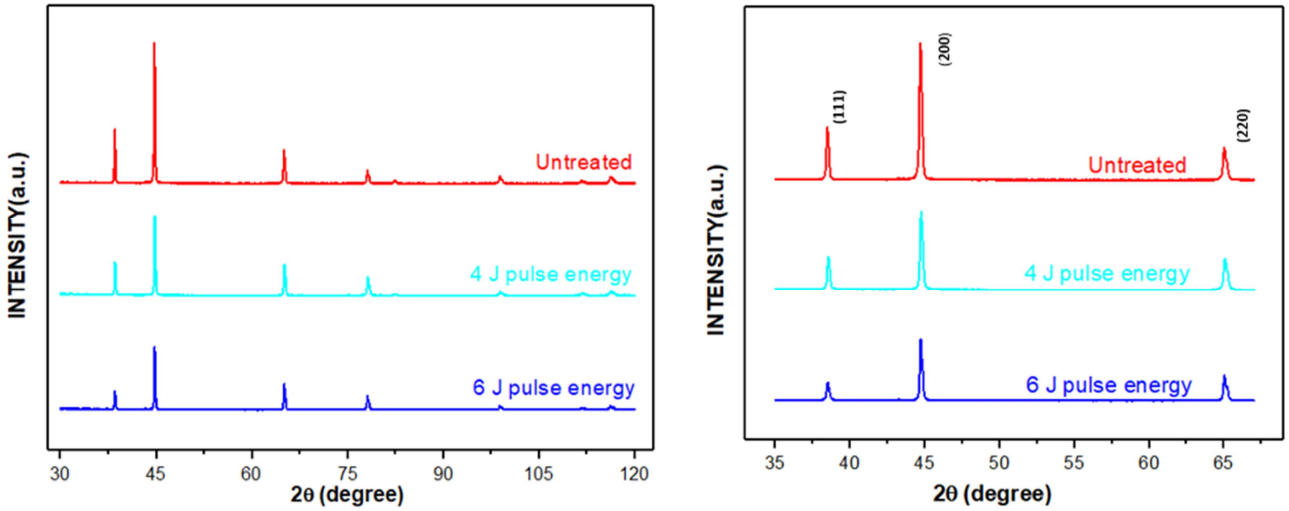

Figure 4. *XRD analysis of untreated and LSP treated AA2024-T351 specimen (a) Indexed graph (b) Magnified graph.*

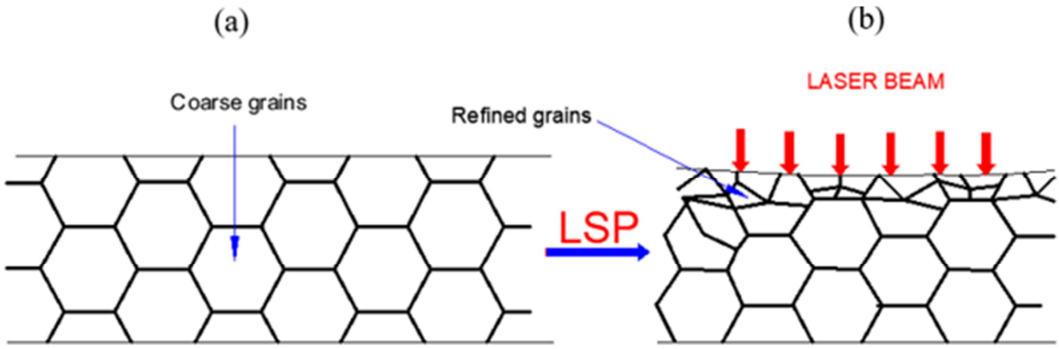

Figure 5. *Schematic illustration of grain evolution after laser shock peening at one surface of a specimen (a) without LSP (b) after LSP.*

3.2. Residual Stress Distribution

During LSP, the specimen is induced with severe plastic deformation leading to the formation of dislocation and new grain boundaries. Besides, high amplitude compressive residual stresses are induced on the surface of the material that enhances its fatigue performance. The measured residual stress distribution curve with and without single laser impact at different pulse energy in depth direction is shown in Figure 6. It can be seen from the figure that the untreated regions are approximately in the zero stress state. This shows that the effect of the initial stress on the shock wave can be ignored [19]. It is evident that LSP introduces great compressive residual stresses layer on the aluminium alloy specimen. The maximum compressive residual stress is found at the treated surface and the value increases with the laser pulse energy. After LSP treatment with 4 J and 6 J pulse energies, the maximum residual stresses are approximately -268 MPa and -334 MPa, respectively. The severe deformation by LSP results from the higher pulse energy. Meanwhile, the value of residual compressive stress decreases gradually with the distance away from the treated surface. The plastically affected depth for the specimen treated with 4 J and 6 J pulse energies are 600 μm and 750 μm respectively.

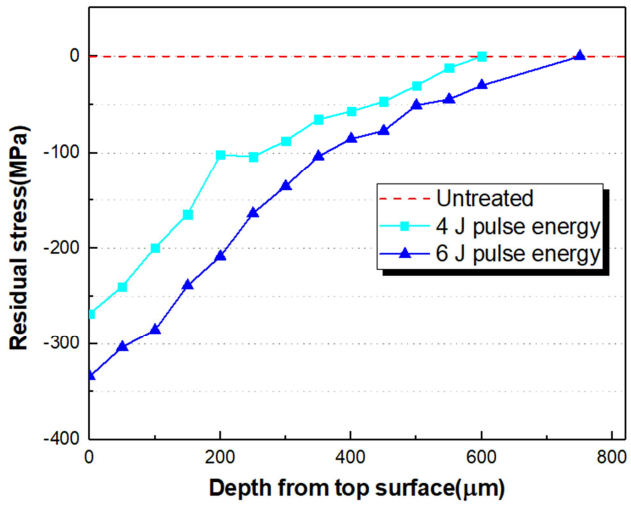

Figure 6. *Residual stress distribution of specimen before and after different LSP pulse energies in depth direction.*

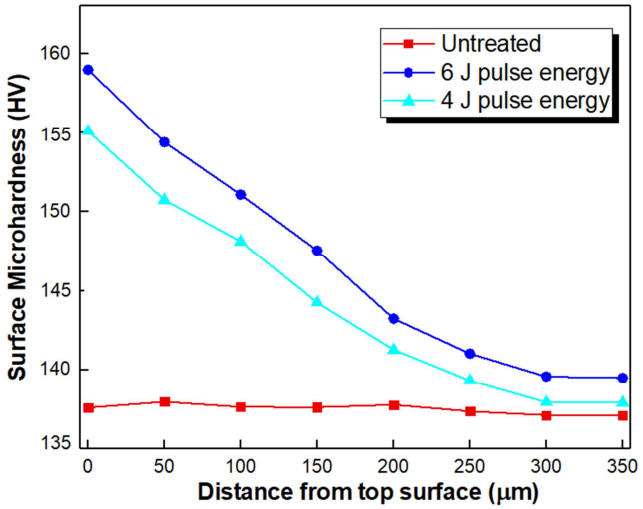

Figure 7. *Microhardness distribution on the cross-section of after different laser energies.*

3.3. Microhardness Analysis

Hardness is a basic mechanical property that is capable of resisting wear, indentation and the prevention of FOD to some extent. The magnitude of microhardness on the specimen surface before and after laser treatment by different pulse energies is shown on Figure 7. The magnitude of microhardness increases effectively with the increase in LSP pulse energy. After laser treatment with pulse energy of 4 J, the microharness increased by 10% from 300 HV (as-received) to 334 HV. With increasing the laser pulse energy to 6 J, the microhardness is 342 HV, showing a 12% increase compared with the untreated specimen. LSP causes severe plastic deformation. Hence, after LSP, the surface microhardness increases mainly due to dislocation strengthening. Also, the microhardness is higher after the higher energy of LSP. The maximum hardness was found at the surface of the material in both cases. And this could be attributed to the induced stresses by the shock wave on the surface of the material. There were severe plastic deformations during LSP that resulted in high dislocation density and strengthening of which lead to the formation of dislocations cells and pinning of dislocation within the material.

3.4. Surface Roughness

The surface roughness and topographical analysis for both treated and untreated specimens are analysed. The surface roughness of the specimen after LSP experienced some changes. It can be observed from Figure 8 that the roughness of the treated sample increased due to ablation and melting especially the specimen treated by 6 J laser pulse energy. The arithmetic average of the absolute values (Ra) of the points along the profile increased from 1.274 μm for the untreated specimen to 1.748 μm and 2.652 μm after irradiating with laser pulse energies of 4 J and 6 J respectively. The uprising of the surface roughness on the specimen can be attributed to LSP and this severe plastic deformation method could be employed to eliminate cracks as a way of increasing the surface area of an implant. The wavy morphology, ablation, height and valley distributions are apparent and evident on all the images in Figures 8(b), (c) and 9 (b), (c). Thus, the influence of LSP is evidently visible on the surface of the alloy.

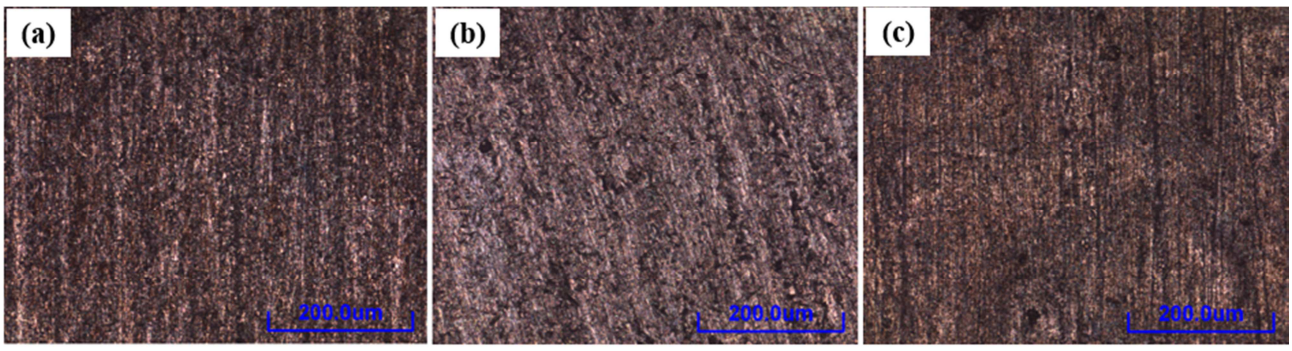

Figure 8. *2D image of AA2024-T351 alloy (a) Untreated specimen (b) LSP treated with 4 J energy (c) LSP treated with 6 J energy.*

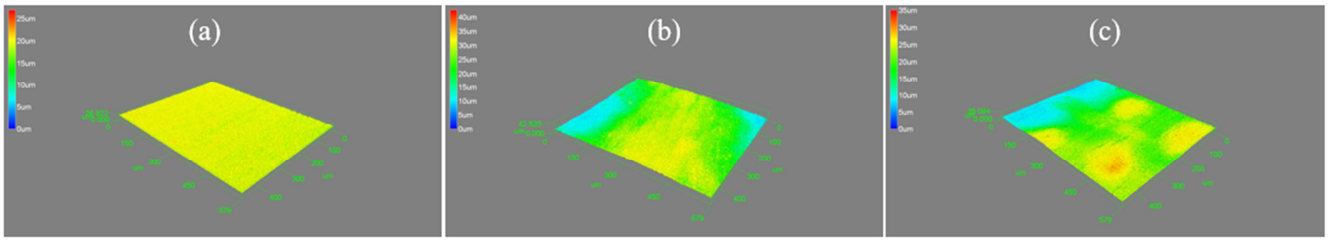

Figure 9. *3D surface profile of AA2024-T351 alloy (a) Untreated specimen (b) LSP treated with 4 J energy (c) LSP treated with 6 J energy.*

4. Conclusion

Based on the experimental investigation of the effects of laser shock peening on mechanical properties and surface morphology of AA2024 alloy by the L-Spiral scanning pattern, the following conclusions can be drawn.

1. With the LSP pulse energy increasing from 4 J to 6 J, the degree of dislocation are enhanced.
2. The roughness of the treated samples increases due to ablation and melting. The specimen treated by 6 J laser pulse energy was significantly affected by ablation than the 4 J pulse energy. The Ra increased from 1.274 µm for the untreated specimen to 1.748 µm and 2.652 µm after the specimen were irradiated with laser pulse energies of 4 J and 6 J respectively.
3. After different LSP pulse energy treatment, the grain size decreased from 125.4 nm to 109.9 nm (4J), and to 95.9 nm (6J). The higher the laser pulse energy is, the more the significance the grain refinement.
4. The microhardness in the impact area increases with the increase of LSP pulse energy and the value of microhardness increases from 137 HV (before LSP) to approximately 155 HV (4 J), and to 158 HV (6 J). Meanwhile, after LSP with different laser pulse energy, the maximum residual stresses are –268 MPa (4 J) and -334 MPa (6 J), and the corresponding plastically affected depths are approximately 600 µm and 750 µm, respectively.

References

[1] Kattoura, M., et al., Effect of laser shock peening on elevated temperature residual stress, microstructure and fatigue behavior of ATI 718Plus alloy. International Journal of Fatigue, 2017. 104: p. 366-378.

[2] Zou, S., et al., Surface integrity and fatigue lives of Ti17 compressor blades subjected to laser shock peening with square spots. Surface and Coatings Technology, 2018. 347: p. 398-406.

[3] Mostafa, A. M., M. F. Hameed, and S. S. Obayya, Effect of laser shock peening on the hardness of AL-7075 alloy. Journal of King Saud University-Science, 2017.

[4] Correa, C., et al., Effect of advancing direction on fatigue life of 316L stainless steel specimens treated by double-sided laser shock peening. International Journal of Fatigue, 2015. 79: p. 1-9.

[5] Ren, X., et al., The effects of residual stress on fatigue behavior and crack propagation from laser shock processing-worked hole. Materials & Design, 2013. 44: p. 149-154.

[6] Granados-Alejo, V., et al., Influence of specimen thickness on the fatigue behavior of notched steel plates subjected to laser shock peening. Optics & Laser Technology, 2017.

[7] Keller, S., et al., Experimental and numerical investigation of residual stresses in laser shock peened AA2198. Journal of Materials Processing Technology, 2017.

[8] Sanchez-Santana, U., et al., Wear and friction of 6061-T6 aluminum alloy treated by laser shock processing. Wear, 2006. 260(7-8): p. 847-854.

[9] Sihai, L., et al., Aluminizing mechanism on a nickel-based alloy with surface nanostructure produced by laser shock peening and its effect on fatigue strength. Surface and Coatings Technology, 2018. 342: p. 29-36.

[10] Wang, J., et al., Effect of laser shock peening on the high-temperature fatigue performance of 7075 aluminum alloy. Materials Science and Engineering: A, 2017. 704: p. 459-468.

[11] Correa, C., et al., Influence of pulse sequence and edge material effect on fatigue life of Al2024-T351 specimens treated by laser shock processing. International Journal of Fatigue, 2015. 70: p. 196-204.

[12] Ganesh, P., et al., Studies on laser peening of spring steel for automotive applications. Optics and Lasers in Engineering, 2012. 50(5): p. 678-686.

[13] Warren, A., Y. Guo, and S. Chen, Massive parallel laser shock peening: simulation, analysis, and validation. International Journal of Fatigue, 2008. 30(1): p. 188-197.

[14] Wang, Y., et al., Energy-level effects on the deformation mechanism in microscale laser peen forming. Journal of Manufacturing Processes, 2007. 9(1): p. 1-12.

[15] Peyre, P., et al., Laser shock processing of aluminium alloys. Application to high cycle fatigue behaviour. Materials Science and Engineering: A, 1996. 210(1-2): p. 102-113.

[16] Standard Test Method for Vickers Hardness of Metallic Materials ASTM International., 2003.

[17] YE, H.-q. and X.-m. FAN, Surface nanocrystallization of 7A04 aluminium alloy induced by circulation rolling plastic deformation. Transactions of Nonferrous Metals Society of China, 2006. 16: p. s656-s660.

[18] Roland, T., et al., Enhanced mechanical behavior of a nanocrystallised stainless steel and its thermal stability. Materials Science and Engineering: A, 2007. 445: p. 281-288.

[19] Altenberger, I., et al., Cyclic deformation and near surface microstructures of shot peened or deep rolled austenitic stainless steel AISI 304. Materials Science and Engineering: A, 1999. 264(1-2): p. 1-16.